2019

DYNAMICS OF THE LATE TRIASSIC ADAMANIAN-REVUELTIAN EXTINCTION, PETRIFIED FOREST NATIONAL PARK, AZ

Reilly F. Hayes
University of Rhode Island, reilly.hayes1@gmail.com

DYNAMICS OF THE LATE TRIASSIC ADAMANIAN-REVUELTIAN EXTINCTION, PETRIFIED FOREST NATIONAL PARK, AZ

BY

REILLY F. HAYES

A THESIS SUBMITTED IN PARTIAL FULFILLMENT OF THE

REQUIREMENTS FOR THE DEGREE OF

MASTER OF SCIENCE

IN

BIOLOGICAL AND ENVIRONMENTAL SCIENCES

UNIVERSITY OF RHODE ISLAND

2019

MASTER OF SCIENCE THESIS

OF

REILLY F. HAYES

APPROVED:

Thesis Committee:

Major Professor David E. Fastovsky

Gavino Puggioni

Simon Engelhart

Nasser H. Zawia
DEAN OF THE GRADUATE SCHOOL

UNIVERSITY OF RHODE ISLAND
2019

ABSTRACT

In the Late Triassic of Petrified Forest National Park (PEFO), AZ, the coincidence of high-precision geochronology and robust lithostratigraphy allows an adaption of the Bayesian statistical approaches of Haslett and Parnell (2008) and Alroy (2014) to quantify the dynamics of a Late Triassic vertebrate extinction and replacement, the Adamanian-Revueltian (A-R) faunal turnover. This analysis indicates negligible probability of synchroneity of Adamanian extinctions and Revueltian originations. This protracted reconstruction of the A-R turnover decouples the event from the geologically instantaneous Manicouagan impact (215.4 $\pm$ 0.20 Ma; Québec, Canada), previously implicated as a causal mechanism.

ACKNOWLEDGMENTS

I would like to thank my committee members, David Fastovsky, Gavino Puggioni, and Simon Engelhart, for the guidance they provided this work. I am grateful to William Parker, Jeffrey Martz, Adam Marsh, and Chuck Beightol for the discussion they have provided throughout this project, and for their work in assembling and maintaining the Petrified Forest National Park fossil database utilized by this study. I would also like to thank Catherine Tiley, Amanda Bednarick, and Samuel Hemmendinger for their assistance with the fieldwork. This work was supported by a Geological Society of America Graduate Student Research Grant, a Paleontological Society Stephen Jay Gould Award, a Rhode Island Space Grant Summer Research Fellowship, a Sigma Xi Grant-in-Aid of Research, and a University of Rhode Island Enhancement of Graduate Research Award.

PREFACE

This thesis is written in Manuscript format, following the formatting guidelines of *Geology*.

TABLE OF CONTENTS

LIST OF TABLES

LIST OF FIGURES

PUBLICATION STATUS

Chapter 1 of this thesis is in preparation for submission to *Geology*. Authors of the submitted manuscript will include Reilly F. Hayes, Gavino Puggioni, William G. Parker, Catherine Tiley, Amanda Bednarick, and David E. Fastovsky.

CHAPTER 1

INTRODUCTION

Extinction dynamics are difficult to quantify because the last appearance of an organism does not likely signify its ultimate extinction (Signor and Lipps, 1982). Major steps towards quantifying the moment of extinction in geological time, by contrast to a last appearance, were taken by Strauss and Sadler (1989), Marshall (1994; 1997), Alroy (2014; 2015), and Solow (1996; 2016), among others (see Wang and Marshall, 2016 for review). Because the required sample sizes and geochronological data are not commonly retrievable, especially from pre-Quaternary deposits, such studies are rarely performed with fossil vertebrates.

This analysis applies Alroy's (2014) Bayesian approach to characterize the Adamanian-Revueltian (A-R) turnover, a Late Triassic vertebrate extinction and replacement exposed in Petrified Forest National Park (PEFO), Arizona, USA (Figure 1.1). Refined dating of Late Triassic Chinle fluvial system in PEFO, in combination with a diverse, stratigraphically controlled vertebrate assemblage, provide the setting for this research. This analysis is particularly apt, as the A-R turnover has been tentatively correlated to the 215.4 $\pm$ 0.20 Ma (Jaret et al., 2018) Manicouagan impact (Dunlavey et al., 2009; Parker and Martz, 2011; Olsen et al., 2011; Onoue et al., 2012; Olsen et al., 2014; Rampino and Caldeira, 2017; Olsen et al., 2018) and the ca. 214.7 Ma aridification of the Chinle (Parker and Martz, 2011; Atchley et al., 2014; Nordt et al., 2015). These initial hypotheses were generated using stratigraphic range plots (Parker and Martz, 2011); this analysis, by contrast, assesses synchroneity of taxon extinctions and originations in time.

The Chinle fluvial system and the Adamanian-Revueltian faunal turnover

The Chinle Formation is a continental, fossiliferous fluvial succession (Blakey and Gubitosa, 1983; Dubiel, 1989, 1992; Trendell et al., 2013). Exposures in PEFO long defied facile stratigraphic interpretation (see Martz and Parker, 2010 for review). This changed with a robust lithostratigraphy (Martz and Parker, 2010), and geochronological analyses producing twelve (Ramezani et al., 2011; Atchley et al., 2014; Nordt et al., 2015) high-precision U-Pb dates through the Chinle Formation.

The Adamanian-Revueltian turnover is now regarded as a transition between two single-taxon biozones, defined by the first appearance datums of species of the pseudopalatine phytosaur *Machaeroprosopus* (Martz and Parker, 2017). This definition supersedes the earlier designation "land vertebrate faunachrons," characterized by successive faunal assemblages at their type localities in the Chinle Formation (Lucas, 1993; Lucas and Hunt, 1993; Lucas and Heckert, 1996; Lucas, 1998; Heckert and Lucas, 2006). Because these assemblages appear distinct within the confines of PEFO (Long and Ballew, 1985; Parker and Martz, 2011), this analysis quantifies the pattern of faunal extinctions and originations there to test synchroneity of the A-R turnover. Adamanian extinctions and Revueltian originations are marked in terms of key constituent taxa: the intersection of extinctions of *Acaenasuchus geoffreyi*, *Trilophosaurus*, *Calyptosuchus wellesi*, *Placerias hesternus*, *Desmatosuchus spurensis*, and *Smilosuchus* defines the Adamanian extinction, while the intersection of originations of *Machaeroprosopus*, *Chindesaurus bryansmalli*, and *Revueltosaurus callenderi* defines the Revueltian origination. These are quantitatively expressed as:

1. $E_{Adamanian} = E_{Acaenasuchus} \cap E_{Trilophosaurus} \cap E_{Calyptosuchus} \cap E_{Placerias} \cap E_{Desmatosuchus} \cap E_{Smilosuchus}$
2. $O_{Revueltian} = O_{Machaeroprosopus} \cap O_{Revueltosaurus} \cap O_{Chindesaurus}$

The hypothesis test is as follows:

H_0: At some time *t* of the total time *T* recorded in the Chinle, there exists a synchronous extinction of Adamanian taxa and origination of Revueltian taxa, e.g.,

$$\exists\, t \in T: E_{Adamanian} \cap O_{Revueltian}$$

H_1: Adamanian extinctions and Revueltian originations were diachronous, e.g.,

$$\neg\exists\, t \in T: E_{Adamanian} \cap O_{Revueltian}$$

METHODS

Dating Adamanian and Revueltian tetrapod faunas in PEFO

Fossil dates were obtained via probabilistic modeling following field correlation to the geochronological dates of Ramezani et al. (2011), Atchley et al. (2014), and Nordt et al. (2015). Although photographs of the original collection sites do not exist (Parker and Martz, 2017), locations of dated zircon samples were obtained from published GPS coordinates (Ramezani et al., 2011, Appendix A) and the positions of beds containing those samples were confirmed in the field by matching the original measured sections (Ramezani et al., 2011, Figure 3) to observed stratigraphic sequences. A close match was found in all cases (Tables 2.1 & 2.2 show the stratigraphic uncertainty associated with each date). Seventy-one fossil localities in PEFO were relocated by GPS, field descriptions, and/or photographic documentation, and then physically correlated to dated beds by walking along continuous beds. This integrated the stratigraphic positions of these localities into the numerical timescale and established the precision of each correlation.

Bayesian geochronological age-depth models (constructed in Bchron, v. 4.3.0, Haslett and Parnell, 2008; Figures 2.1 & 2.2) of the Chinle Formation next generated 1000 possible ages for each locality. Bchron defines a distribution of plausible ages for each stratigraphic level, constructed from a suite (in this case, 1000) of stochastically interpolated chronologies which delimit age envelopes for the stratigraphic thickness between each pair of dates. Additional age distributions were constructed for a floral turnover constrained to a 2.3 m stratigraphic interval around a distinctive red silcrete (*sensu* Martz and Parker, 2010) in the Sonsela Member

(Reichgelt et al., 2013; Baranyi et al., 2017). Also included were fossils from two additional localities: the nearby *Placerias* Quarry (Camp and Welles, 1956), dated with a zircon sample collected from the fossiliferous bed (Ramezani et al., 2014), and the Hayden Quarry (Irmis et al., 2011). A single date from the Hayden Quarry with significant analytical uncertainty ($\pm$ 0.7 Ma) accommodated a broad range of possible ages for fossils, likely encompassing the complete depositional age of the Quarry.

Analytical error came from three sources: the geochronological precision of the dates (Ma), the stratigraphic positions of the zircon samples (m), and the correlations of dates with fossil localities (m). The geochronological precision of the dates is described by the "*X"* error of Ramezani et al. (2011, Supplement, Table S1), because they represent the work of a single lab (MIT's EarthTime laboratory) in a single isotopic system (U-Pb). This uncertainty is generally $\leq$ 0.1%. Because the precision of each fossil position varied with the robustness of its correlation to the dated beds (see Table 2.7), the age-depth model estimates ages more conservatively for less precisely correlated fossil localities.

Quantifying extinctions and replacements in time using Bayesian arguments

Alroy (2014) proposed Bayesian arguments to estimate extinction times (as distinct from last appearance times), stated as a conditional (posterior) probability: what is the chance that a species has gone extinct conditional on the fact that it has not been observed after a certain time?

Following his method, a sequence of 0.1 Ma time "bins" was first constructed in which to evaluate extinction probability. These bins were populated with fossils according to the age-depth models; data for each taxon thus consisted of 1000

sequences of successes or failures to observe that taxon through the full succession of bins.

The Alroy (2014) method ultimately produces a posterior probability distribution of extinction for each taxon. This first requires (1) a sampling probability, or the frequency of findings over the observation range, and (2) a prior probability. Sampling probability was defined with four components, for which n_p gives the time where a taxon is present, and n_a gives the time where that taxon is absent:

1. The probability of observing a certain taxon if the taxon is not extinct is given by the frequency over the observed range minus the first and last sighting:

   $P(D|\bar{E}) = \frac{n_p - 2}{n_p + n_a - 2}$

2. The probability of not observing a certain taxon if the taxon is not extinct is

   $P(\bar{D}|\bar{E}) = 1 - P(D|\bar{E})$

3. The probability of observing a certain taxon if the taxon is extinct is

   $P(D|E) = 0$

4. The probability of not observing a certain taxon if the taxon is extinct is

   $P(\bar{D}|E) = 1 - P(D|E) = 1$

Definition of the prior probability $P(E)$, or probability of extinction at any point in time, followed the assumptions of Alroy (2014): (a) that the probability of an organism having gone extinct can be modeled exponentially (i.e. longer the elapsed time beyond the last fossil, the greater the chance that the extinction has already occurred), and (b) because it cannot be known whether the organism is better considered extinct or extant at the time of the last fossil, the chance of extinction there

is best considered 50%. Indicating with R the observed range of a given taxon, the prior $P(E)$ was thus specified as follows:

$$P(E) = -\log(0.5)/R$$

To accommodate the possibility of strong dissonance between the observed and true range of a taxon (dubbed "undersampling" by Alroy [2014]), analyses were also run in which the denominator of $P(E)$ was doubled to make the algorithm more conservative.

Posterior extinction probability, or probability that a taxon is extinct given that a sighting is not recorded, was next calculated using Bayes' Theorem. Because the goal was to assess the probability of extinction at different points in time, the posterior probability at time *t* became part of the prior for the next time interval *t+1*. Let:

1. $P(A_t) = P(E_t|\bar{D}_t) + \left(1 - P(E_t|\bar{D}_t)\right)P(E)$
2. $P(B_t) = (1 - P(E_t|\bar{D}_t))(1 - P(E))(1 - P(D_t|\bar{E}_t))$

The iterative, posterior-dependent formula to evaluate the probability of extinction was thus as follows:

$$P(E_{t+1}|\bar{D}_{t+1}) = \frac{P(A_t)}{P(A_t) + P(B_t)}$$

This operation was repeated to calculate, for each taxon, posterior extinction probability for each sequence of probabilistic age-depth relationships. Because the relative ages of fossil localities varied across each sequence, calculations accommodate the possibility that fossil ages do not strictly adhere to stratigraphic superposition, as might occur in a fluvial system.

Testing for synchroneity of extinctions and originations

To test that extinctions were synchronous, an average posterior extinction probability of each taxon in each bin was calculated from all 1000 sequences. Because the analysis assumed that the extinction of each Adamanian taxon occurred at some point within the analytical time series, a posterior extinction probability density was defined for each taxon by scaling per-bin probabilities such that $\sum_{t=1}^{153} P(E_t|\overline{D}_t) = 1$. The joint probability that *n* taxa went extinct at any time *t* is the intersection of their posterior extinction probability densities at that time. The overall probability that these *n* taxa went extinct synchronously at any time *t* was therefore defined as the summation of these joint taxic probabilities:

$$P(E_1|\overline{D}_1) \cap \ldots P(E_n|\overline{D}_n) = \sum_{t=1}^{153} P\left(E_{1_t}\middle|\overline{D}_{1_t}\right) \ldots P\left(E_{n_t}\middle|\overline{D}_{n_t}\right)$$

This operation assumed conditional independence of taxon extinctions. This assumption is practical, as hypothetical dependencies can be neither demonstrated nor falsified.

Analytical treatment of Revueltian originations mirrored that of extinctions: following Alroy (2014), all of the operations above were performed in reverse from the first fossil occurrence of a taxon to calculate posterior origination probability.

RESULTS

Based on all available evidence, model support for a synchronous A-R turnover is negligible (Table 1.1). Regarded individually, the probabilities of a synchronous Adamanian extinction and Revueltian origination are also slim. However, pairwise comparisons between taxon extinctions and originations (Table 1.2) indicate modest support for synchroneity of some biotic events.

DISCUSSION AND CONCLUSIONS

Two possible causes of the A-R turnover have been proposed in the literature. Many authors (Dunlavey et al., 2009; Parker and Martz, 2011; Olsen et al., 2011; Onoue et al., 2012; Olsen et al., 2014; Rampino and Caldeira, 2017; Olsen et al., 2018) preliminarily linked it with the Manicouagan impact structure of Québec, Canada. Alternatively, Parker and Martz (2011), Atchley et al. (2014), and Nordt et al. (2015) suggested climatic aridification as a possible mechanism driving the event, as signified by the appearance of abundant pedogenic carbonate, the dominance of well-drained paleosols (Atchley et al., 2014; Nordt et al., 2015), and smectite-dominated sandstone clay mineral assemblages (Jin et al., 2018) in the upper Sonsela Member of the Chinle. However, the near-coincidence of this climatic shift (no later than ca. 214.7 Ma) and the Manicouagan impact (215.40 $\pm$ 0.20 Ma; Jaret et al., 2018) confounds these extinction mechanisms *a priori*. The essential question is therefore whether the pattern of extinctions and originations conforms to classes of extinction mechanisms, operating on disparate time scales, plausibly associated with each event.

Since the Alvarez et al. (1980) attribution of the Cretaceous-Paleogene (K-Pg) mass extinction to an asteroid impact, it has been universally recognized that impact-driven extinctions must be synchronous and abrupt (i.e. the "short, sharp, shock" of Clemens et al., 1981 [after W.S. Gilbert]). Because this analysis strongly supports diachronous Adamanian extinctions, the Manicouagan impact does not likely represent the dominant cause of the event. These data, however, do not disqualify the impact from some effect on Chinle ecosystems, as posterior probability of some taxon extinctions—and most strikingly, a floral turnover (Reichgelt et al., 2013; Baranyi et

al., 2017)—is not insignificant at the time (Table 2). Several of these taxa (*Desmatosuchus spurensis, Placerias hesternus,* and *Smilosuchus*) represent not only genera, but complete clades that are lost in western North America at that time (i.e., Dematosuchia, Dicynodontia, and non-mystriosuchian phytosaurs). While the data reported here suggest a decoupling from a marine extinction attributed to the impact (Onoue et al., 2016), the loss of these clades would indicate that something of significance occurred in the terrestrial realm as well. The model presented here cannot reject some effect of the Manicouagan impact on Chinle ecosystems, but available geochronological and fossil data indicate a pattern of extinctions and originations for which it cannot be plausibly assigned responsibility: there is no "short, sharp, shock."

The final ca. 214.7 Ma collapse of the Late Triassic megamonsoon system in western equatorial Pangea lagged behind a shift of mean annual precipitation (MAP) from humid to subhumid conditions (Nordt et al., 2015). The last observed occurrences of *Acaenasuchus geoffreyi, Calyptosuchus wellesi, Trilophosaurus, Placerias hesternus, Desmatosuchus spurensis* and *Smilosuchus gregorii* all precede the stratigraphic dominance of pedogenic carbonate lenses cited as stratigraphic evidence of the collapse (Parker and Martz, 2011; Nordt et al. 2015). However, the sparseness of climate data between ca. 218.0 Ma and ca. 214.7 Ma obscures the nature of this shift during an interval in which the extinctions of most of these taxa are probable. Climate change thus remains a plausible mechanism underpinning the A-R turnover, but the asynchronous pattern of extinctions and originations best supported by this analysis suggests that a geologically instantaneous biotic response to final monsoonal collapse is improbable.

REFERENCES

Alroy, J., 2014, A simple Bayesian method of inferring extinction: Paleobiology v. 40, no. 4, p. 584–607, https://doi.org/10.1666/13074.

Alroy, J., 2015, Current extinction rates of reptiles and amphibians: Proceedings of the National Academy of Sciences USA, v. 112, no. 42, p. 13003-13008, https://doi.org/10.1073/pnas.1508681112.

Alvarez, L.W., Alvarez, W., Asaro, F., and Michel, H.V., 1980, Extraterrestrial cause for the Cretaceous-Tertiary extinction: Science, v. 208, no. 4448, p. 1095-1108, https://doi.org/10.1126/science.208.4448.1095.

Atchley S.C., Nordt L.C., Dworkin S.I., Ramezani J., Parker W.G., Ash S.R., and Bowring S.A., 2014, A linkage among Pangean tectonism, cyclic alluviation, climate change, and biologic turnover in the Late Triassic: The record from the Chinle Formation, southwestern United States: Journal of Sedimentary Research, v. 83, no. 12, p. 1147-1161, https://doi.org/10.2110/jsr.2013.89.

Baranyi, V., Reichgelt, T., Olsen, P.E., Parker, W.G., and Kürschner, W.M., 2017, Norian vegetation history and related environmental changes: New data from the Chinle Formation, Petrified Forest National Park (Arizona, SW USA): GSA Bulletin, v. 130, no. 5-6, p. 775-795, https://doi.org/10.1130/B31673.1.

Blakey, R.C., and Gubitosa, R., 1983, Late Triassic paleogeography and depositional history of the Chinle Formation, southeastern Utah and northern Arizona, *in* Reynolds, M.W., and Dolly, E.D., eds., Mesozoic Paleogeography of West-Central United States: Denver, Colorado, Rocky Mountain Section SEPM, p. 57-76.

Camp, C., and Welles, S.P., 1956, *Triassic Dicynodont Reptiles*: Memoirs of the University of California, University of California Press, Berkeley, CA, v. 13, p. 255 - 348.

Clemens, W.A., Archibald, J.D., and Hickey, L.J., 1981, Out with a whimper not a bang: Paleobiology v. 7, no. 3, p. 293-298, https://doi.org/10.1017/s0094837300004589.

Dubiel, R.F., 1989, Depositional and climatic setting of the Upper Triassic Chinle Formation, Colorado Plateau, *in* Lucas, S.G., and Hunt, A.P., eds., Dawn of the Age of the Dinosaurs in the American Southwest: Albuquerque, New Mexico, New Mexico Museum of Natural History, p. 171-187.

Dubiel, R.F., 1992, Sedimentology and depositional history of the Upper Triassic Chinle Formation in the Uinta, Piceance, and Eagle Basins, northwestern Colorado and northeastern Utah: U.S. Geological Survey Bulletin 1787-W, 25 p., https://doi.org/10.3133/b1787W.

Dunlavey, M.G., Whiteside, J.H., and Irmis, R.B., 2009, Ecosystem instability during the rise of the dinosaurs: Evidence from the Late Triassic in New Mexico and Arizona: Geological Society of America Abstracts with Programs, v. 41, no. 7, p. 477.

Fastovsky, D.E., and Bercovici, A., 2016, The Hell Creek Formation and its contribution to the Cretaceous–Paleogene extinction: A short primer: Cretaceous Research, v. 57, p. 368-390, https://doi.org/10.1016/j.cretres.2015.07.007.

Haslett, J., and Parnell, A.C., 2008, A simple monotone process with application to radiocarbon-dated depth chronologies: Journal of the Royal Statistical Society:

Series C (Applied Statistics), v. 57, no. 4, p. 399-418, https://doi.org/10.1111/j.1467-9876.2008.00623.x.

Heckert, A.B., and Lucas, S.G., 2006, Micro- and small vertebrate biostratigraphy and biochronology of the Upper Triassic Chinle Group, southwestern USA: Bulletin of the New Mexico Museum of Natural History and Science, v. 37, p. 94–104.

Irmis, R.B., Nesbitt, S.J., Padian, K., Smith, N.D., Turner, A.H., Woody, D., and Downs, A., 2007, A Late Triassic dinosaurimorph assemblage from New Mexico and the rise of dinosaurs: Science, v. 317, p. 358-361, https://doi.org/10.1126/science.1143325.

Jaret, S.J., Hemming, S.R., Rasbury, E.T., Thompson, L.M., Glotch, T.D., Ramezani, J.R., and Spray, J.G., 2018, Context matters – Ar–Ar results from in and around the Manicouagan Impact Structure, Canada: Implications for martian meteorite chronology: Earth and Planetary Science Letters, v. 501, p. 78-89, https://doi.org/10.1016/j.epsl.2018.08.016.

Jin, C., Dworkin, S., Atchley, S., and Nordt, L., 2018, Eogenetic diagenesis of Chinle sandstones, Petrified Forest National Park (Arizona, USA): A record of Late Triassic climate change: Sedimentology, v. 65, p. 1277-1300, https://doi.org/10.1111/sed.12421.

Long, R.A., and Ballew, K.L., 1985, Aetosaur dermal armor from the late Triassic of southwestern North America, with special reference to material from the Chinle Formation of Petrified Forest National Park: Museum of Northern Arizona Bulletin, v. 54, p. 45–68.Lucas, S.G., 1993, The Chinle Group: Revised stratigraphy and biochronology of Upper Triassic nonmarine strata in the western

United States: Museum of Northern Arizona Bulletin, v. 59, p. 27–50.

Lucas, S.G.,1998, Global Triassic tetrapod biostratigraphy and biochronology: Palaeogeography, Palaeoclimatology, Palaeoecology, v. 143, p. 347-384, https://doi.org/10.1016/s0031-0182(98)00117-5.

Lucas, S.G., and Heckert, A.B., 1996, Vertebrate biochronology of the Late Triassic of Arizona: Proceedings of the Fossils of Arizona Symposium, v. 4, p. 63–81.

Lucas, S.G., and Hunt, A.P., 1993, Tetrapod biochronology of the Chinle Group (Upper Triassic), western United States: Bulletin of the New Mexico Museum of Natural History and Science, v. 3, p. 327–329.

Marshall, C.R., 1994, Confidence intervals on stratigraphic ranges: partial relaxation of the assumption of randomly distributed fossil horizons: Paleobiology, v. 20, no. 4, p. 459–469, https://doi.org/10.1017/s0094837300012938.

Marshall C.R., 1997, Confidence intervals on stratigraphic ranges with nonrandom distributions of fossil horizons: Paleobiology, v. 23, no. 2, p. 165-173, https://doi.org/10.1017/s0094837300016766.

Martz, J.W. and Parker, W.G., 2010, Revised lithostratigraphy of the Sonsela Member (Chinle Formation, Upper Triassic) in the southern part of Petrified Forest National Park, Arizona: PLoSONE, v. 5, no. 2, e9329, https://doi.org/10.1371/journal.pone.0009329.

Martz, J.W., and Parker, W.G., 2017, Revised formulation of the Late Triassic Land Vertebrate “Faunachrons” of western North America: recommendations for codifying nascent systems of vertebrate biochronology, *in* Zeigler, K., and Parker, W.G., eds., Terrestrial depositional systems: deciphering complexities through

multiple stratigraphic methods: Amsterdam, Netherlands, Elsevier, p. 39–125, https://doi.org/10.1016/b978-0-12-803243-5.00002-9.

Nordt, L., Atchely, S., and Dworkin, S., 2015, Collapse of the late Triassic megamonsoon in western equatorial Pangea, present-day American Southwest: Geological Society of America Bulletin, v. 127, no. 11-12, p. 1798 – 1815, https://doi.org/10.1130/b31186.1.

Olsen, P.E., Geissman, J., Gehrels, G., Irmis, R., Kent, D., Mundil, R., Parker, W., Sha, J., Molina-Garza, R., Kürschner, W., and Bachmann, G., 2014, The Colorado Plateau Coring Project (CPCP): Chronostratigraphic context for Triassic-Jurassic Earth system events and processes: Abstracts of the 4th International Palaeontological Congress, Mendoza, Argentina, UNESCO-IUGS ICGP 632, p. 878.

Olsen, P.E., Geissman, J.W., Kent, D.V., Gehrels, G.E., Mundil, R., Irmis, R.B., Lepre, C., Rasmussen, C., Giesler, D., Parker, W.G., Zakharaova, N., Kürschner, W., Miller, C., Baranyi, V., Schaller, M.F., Whiteside, J.H., Schnurrenberger, D., Noren, A., Shannon, K.B., O'Grady, R., Colbert, M.W., Maisano, J., Edey, D., Kinney, S.T., Molina-Garza, R., Bachman, G.H., Sha, J., and the CPCD team, 2018, Colorado Plateau Coring Project, Phase I (CPCP-I): a continuously cored, globally exportable chronology of Triassic continental environmental change from western North America: Scientific Drilling, v. 24, p. 15-40, https://doi.org/10.5194/sd-24-15-2018.

Olsen, P.E., Kent, D.V., and Whiteside, J.H., 2011, Implications of the Newark Supergroup-based astrochronology and geomagnetic polarity time scale (Newark-

APTS) for the tempo and mode of the early diversification of the Dinosauria: Earth and Environmental Science Transactions of the Royal Society of Edinburgh, v. 101, no. 3-4, p. 201-229, https://doi.org/10.1017/s1755691011020032.

Onoue, T., Sato, H., Nakamura, T., Noguchi, T., Hidaka, Y., Shirai, N., Ebihara, M., Osawa, T., Hatsukawa, Y., Toh, Y., Koizumi, M., Harada, H., Orchard, M.J., and Nedachi, M., 2012, Deep-sea record of impact apparently unrelated to mass extinction in the Late Triassic: Proceedings of the National Academy of Sciences USA, v. 109, no. 47, p. 19134-19139, https://doi.org/10.1073/pnas.1209486109.

Onoue, T., Sato, H., Yamashita, D., Ikehara, M., Yasukawa, K., Fujinaga, K., Kato, Y., and Matsuoka, A., 2016, Bolide impact triggered the Late Triassic extinction event in equatorial Panthalassa: Scientific Reports, v. 6, p. 29609, https://doi.org/10.1038/srep29609.

Parker, W.G., and Martz, J.W., 2011, The Late Triassic (Norian) Adamanian-Revueltian tetrapod faunal transition in the Chinle Formation of Petrified Forest National Park, Arizona: Earth and Environmental Science Transactions of the Royal Society of Edinburgh, v. 101, no. 3–4, p. 231–260, https://doi.org/10.1017/s1755691011020020.

Parker, W.G., and Martz, J.W., 2017, Building local biostratigraphic models for the Upper Triassic of Western North America: Methods and Considerations, *in* Zeigler, K., and Parker, W.G., eds., Terrestrial depositional systems: deciphering complexities through multiple stratigraphic methods: Amsterdam, Netherlands, Elsevier, p. 1-38, https://doi.org/10.1016/b978-0-12-803243-5.00001-7.Ramezani J., Hoke G.D., Fastovsky D.E., Bowring S.A., Therrien F., Dworkin S.I., Atchley

S.C., and Nordt L.C., 2011, High-precision U-Pb zircon geochronology of the Late Triassic Chinle Formation, Petrified Forest National Park (Arizona, USA): Temporal constraints on the early evolution of dinosaurs: Geological Society of America Bulletin, v. 123 no. 11-12, p. 2142-2159, https://doi.org/10.1130/b30433.1.

Ramezani, J., Fastovsky, D.E., and Bowring, S.A., 2014, Revised chronostratigraphy of the lower Chinle Formation strata in Arizona and New Mexico (USA): High-precision U-Pb geochronological constraints on the Late Triassic evolution of dinosaurs: American Journal of Science, v. 314, p. 981-1008, https://doi.org/10.2475/06.2014.01.

Rampino, M.R., and Caldeira, K., 2017, Correlation of the largest craters, stratigraphic impact signatures, and extinction events over the past 250 Myr: Geoscience Frontiers, v. 8, no. 6, p. 1241-1245, https://doi.org/10.1016/j.gsf.2017.03.002.

Reichgelt, T., Parker, W.G., Martz, J.W., Conran, J.G., van-Konijnenburg-van Cittert, J.H.A., and Kürschner, W.M., 2013, The palynology of the Sonsela Member (Late Triassic, Norian) at Petrified Forest National Park, USA: Review of Palaeobotany and Palynology, v. 189, p. 18-28, https://doi.org/10.1016/j.revpalbo.2012.11.001.

Signor, P.W. III, and Lipps, J.H., 1982, Sampling bias, gradual extinction patterns and catastrophes in the fossil record, *in* Silver, L.T., and Schultz, P.H., eds., Geological Implications of Large Asteroids and Comets on the Earth: Geological Society of America Special Paper no. 190, p. 291 – 296, https://doi.org/10.1130/spe190-p291.

Solow, A.R., 1996, Tests and confidence intervals for a common upper endpoint in fossil taxa: Paleobiology, v. 22, no. 3, p. 406-410,

https://doi.org/10.1017/s0094837300016353.

Solow, A.R., 2016, A simple Bayesian method of inferring extinction: comment: Ecology, v. 97, no. 3, p. 796-798, https://doi.org/10.1890/15-0336.1.

Strauss, D. and Sadler, P.M., 1989, Classical confidence intervals and Bayesian probability estimates for ends of local taxon ranges: Mathematical Geology, v. 21, no. 4, p. 411-427, https://doi.org/10.1007/bf00897326.

Trendell, A.M., Atchley, S.C., and Nordt, L.C., 2013, Facies analysis of a probable large-fluvial-fan depositional system: The Upper Triassic Chinle Formation at Petrified Forest National Park, Arizona, USA: Journal of Sedimentary Research, v. 83, p. 873-895, https://doi.org/10.2110/jsr.2013.55.

Wang, S.C., and Marshall, C.R., 2016, Estimating times of extinction in the fossil record: Biology Letters, v.12, https://doi.org/10.1098/rsbl.2015.0989.

TABLES AND FIGURES

Table 1.1. Posterior probability of synchronous Adamanian extinctions, Revueltian originations, and Adamanian-Revueltian faunal turnover. Probability given undersampling (see Methods) in parentheses.

Event	Posterior Probability
$E_{Adamanian}$	$1.22\ x\ 10^{-10}$ ($2.02\ x\ 10^{-10}$)
$O_{Revueltian}$	$4.52\ x\ 10^{-4}$ ($2.93\ x\ 10^{-4}$)
$E_{Adamanian} \cap O_{Revueltian}$	$5.51\ x\ 10^{-14}$ ($5.91\ x\ 10^{-14}$)

Table 1.2. Probability of synchroneity of paired Chinle biotic events. Probability of synchroneity with Manicouagan impact is posterior probability at 215.40 ± 0.20 Ma; all others are summation of joint probabilities across full time series. Probability given undersampling (see Methods) in parentheses.

Event	*Acaenasuchus* Extinction	*Trilophosaurus* Extinction	*Calyptosuchus* Extinction	*Placerias* Extinction	Desmatosuchus Extinction	*Smilosuchus* Extinction	*Typothorax* Origination	*Paratypothorax* Origination	*Machaeroprosopus* Origination	*Revueltosaurus* Origination	*Chindesaurus* Origination	Floral Turnover	Manicouagan Impact
Acaenasuchus Extinction		1.37% (1.15%)	1.44% (1.23%)	1.44% (1.23%)	0.89% (0.98%)	0.79% (0.96%)	0.55% (0.81%)	0.02% (0.01%)	0.21% (0.07%)	1.14% (1.27%)	1.29% (1.06%)	1.32% (1.16%)	1.36% (1.34%)
Trilophosaurus Extinction	1.37% (1.15%)		1.60% (1.34%)	1.04% (1.09%)	0.92% (1.08%)	0.61% (0.87%)	0.01% (0.00%)	0.09% (0.03%)	1.36% (1.43%)	1.42% (1.07%)	1.48% (1.21%)	1.64% (1.54%)	7.87% (7.88%)
Calyptosuchus Extinction	1.44% (1.23%)	1.60% (1.34%)		1.10% (1.06%)	0.86% (0.95%)	0.43% (0.59%)	0.01% (0.00%)	0.03% (0.01%)	1.50% (1.81%)	1.66% (1.34%)	1.76% (1.55%)	2.08% (2.16%)	9.55% (11.08%)
Placerias Extinction	0.89% (0.98%)	1.04% (1.09%)	1.10% (1.06%)		1.51% (1.50%)	1.35% (1.51%)	0.00% (0.00%)	0.00% (0.00%)	1.60% (1.14%)	1.12% (0.62%)	1.26% (0.74%)	1.60% (1.15%)	8.59% (6.29%)
Desmatosuchus Extinction	0.79% (0.96%)	0.92% (1.08%)	0.86% (0.95%)	1.51% (1.50%)		1.67% (1.74%)	0.00% (0.00%)	0.00% (0.00%)	1.75% (1.02%)	0.93% (0.43%)	1.08% (0.52%)	1.25% (0.79%)	7.89% (4.91%)
Smilosuchus Extinction	0.55% (0.81%)	0.61% (0.87%)	0.43% (0.59%)	1.35% (1.51%)	1.67% (1.74%)		0.00% (0.00%)	0.00% (0.00%)	0.87% (0.39%)	0.33% (0.14%)	0.38% (0.16%)	0.26% (0.16%)	1.24% (0.78%)
Typothorax Origination	0.02% (0.01%)	0.01% (0.00%)	0.01% (0.00%)	0.00% (0.00%)	0.00% (0.00%)	0.00% (0.00%)		1.97% (1.88%)	0.01% (0.02%)	0.19% (0.30%)	0.10% (0.17%)	0.00% (0.00%)	0.00% (0.00%)
Paratypothorax Origination	0.21% (0.07%)	0.09% (0.03%)	0.03% (0.01%)	0.00% (0.00%)	0.00% (0.00%)	0.00% (0.00%)	1.97% (1.88%)		0.02% (0.03%)	0.24% (0.34%)	0.15% (0.21%)	0.00% (0.00%)	0.02% (0.01%)
Machaeroprosopus Origination	1.14% (1.27%)	1.36% (1.43%)	1.50% (1.81%)	1.60% (1.14%)	1.75% (1.02%)	0.87% (0.39%)	0.01% (0.02%)	0.02% (0.03%)		1.82% (1.46%)	2.08% (1.73%)	2.43% (2.74%)	14.69% (15.96%)
Revueltosaurus Origination	1.29% (1.06%)	1.42% (1.07%)	1.66% (1.34%)	1.12% (0.62%)	0.93% (0.43%)	0.33% (0.14%)	0.19% (0.30%)	0.24% (0.34%)	1.82% (1.46%)		1.88% (1.51%)	2.33% (1.81%)	12.49% (8.88%)
Chindesaurus Origination	1.32% (1.16%)	1.48% (1.21%)	1.76% (1.55%)	1.26% (0.74%)	1.08% (0.52%)	0.38% (0.16%)	0.10% (0.17%)	0.15% (0.21%)	2.08% (1.73%)	1.88% (1.51%)		2.69% (2.25%)	15.01% (11.40%)
Floral Turnover	1.36% (1.34%)	1.64% (1.54%)	2.08% (2.16%)	1.60% (1.15%)	1.25% (0.79%)	0.26% (0.16%)	0.00% (0.00%)	0.00% (0.00%)	2.43% (2.74%)	2.33% (1.81%)	2.69% (2.25%)		34.08%
Manicouagan Impact	6.36% (6.67%)	7.87% (7.88%)	9.55% (11.08%)	8.59% (6.29%)	7.89% (4.91%)	1.24% (0.78%)	0.00% (0.00%)	0.02% (0.01%)	14.69% (15.96%)	12.49% (8.88%)	15.01% (11.40%)	34.08%	

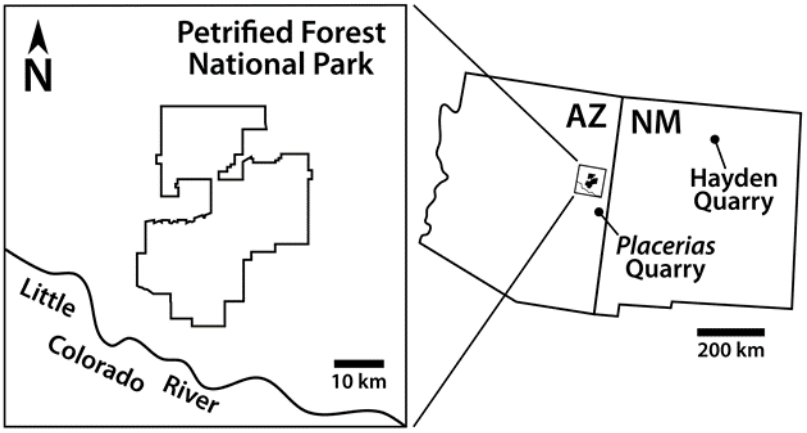

Figure 1.1. Locations of Petrified Forest National Park, *Placerias* Quarry, and Hayden Quarry in Arizona (AZ) and New Mexico (NM).

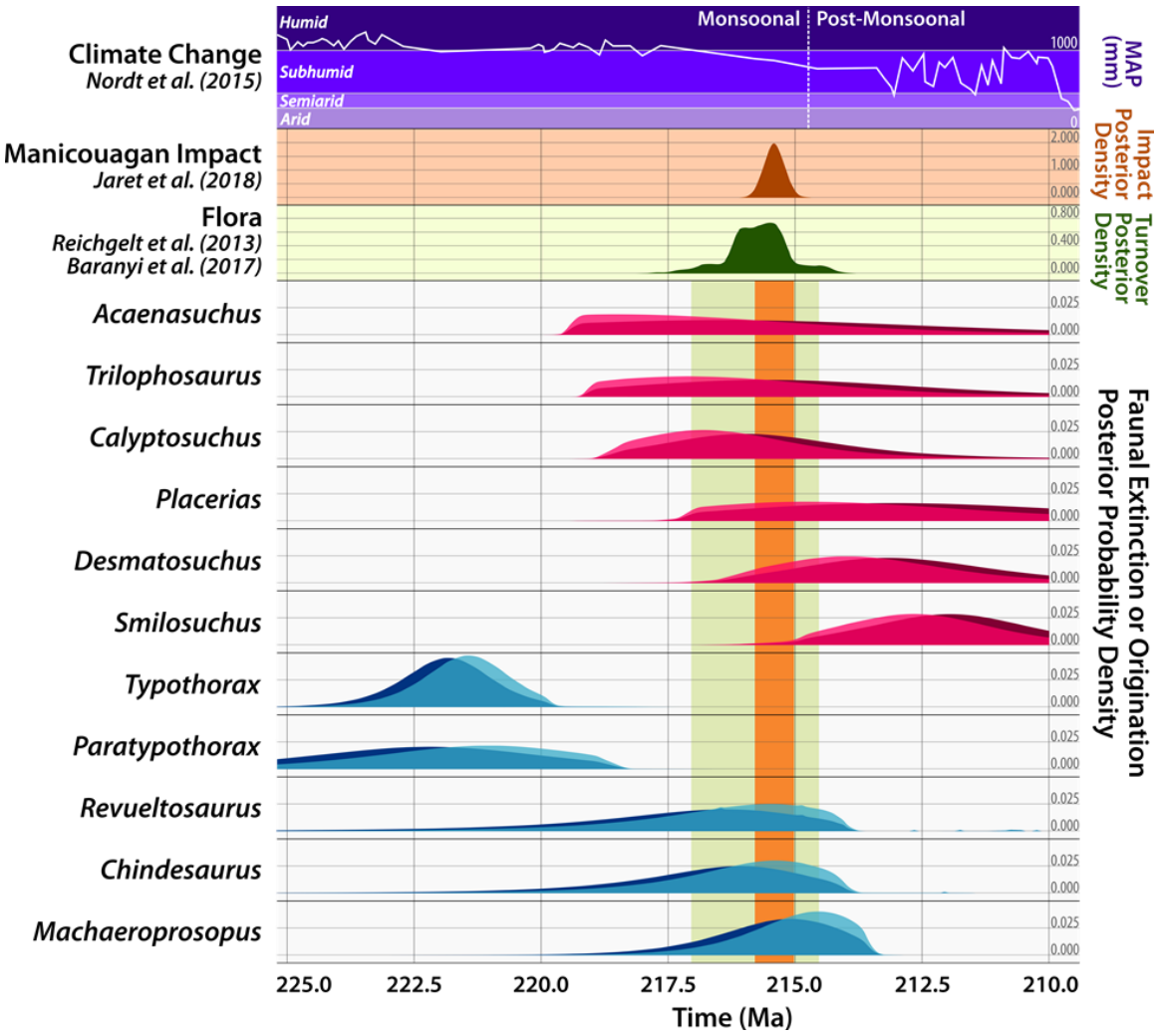

Figure 1.2. Posterior probability density functions of extinction and origination produced by Alroy (2014) algorithm, applied in 1000 simulations to 11 tetrapod taxa. Pink and blue densities respectively refer to extinction and origination. Dark-colored, opaque densities are obtained under assumption of "undersampling"; light, translucent densities are not (see Methods). Chinle mean annual precipitation (MAP) record of Nordt et al. (2015) shown above. Also above are posterior probability densities of floral turnover (green; Reichgelt et al., 2013; Baranyi et al., 2017) and Manicouagan impact (orange); vertically-oriented green and orange fields (below) delineate respective 95% highest posterior density regions.

PUBLICATION STATUS

Chapter 2 of this thesis will serve as a Supplement to Chapter 1 when that manuscript is submitted to *Geology*. It will not be published independently of Chapter 1 elsewhere.

CHAPTER 2

NOTES ON TAXON SAMPLING

Diagnoses of fossils used in this analysis are current as of Summer 2018. As Parker and Martz (2011) observe, many taxa in the Chinle of Petrified Forest National Park (PEFO) persist through the Adamanian-Revueltian (A-R) faunal turnover: these include Crocodylomorpha, Coelophysoidea, Rauisuchidae, Shuvosauridae, Silesauridae, Sphenosuchia, *Vancleavea*, and *Koskinonodon perfectus*, following the recognition of Gee et al. (2017) and Gee and Parker (2017) that *Apachesaurus gregorii* likely represents a juvenile of this taxon. Because these taxa are not thought to originate or go extinct within the analytical time series, they were excluded from this analysis.

The Adamanian faunal assemblage is comprised by *Acaenasuchus geoffreyi*, *Trilophosaurus*, *Calyptosuchus wellesi*, *Placerias hesternus*, *Desmatosuchus spurensis*, *Smilosuchus*, *Scutarx deltatylus*, *Poposaurus*, *Adamanasuchus*, *Tecovasuchus*, *Acallosuchus*, *Crosbysaurus*, and *Malerisaurus*, while the Revueltian assemblage is comprised by *Machaeroprosopus*, *Chindesaurus bryansmalli*, *Revueltosaurus callenderi*, and *Rioarribasuchus*. Additionally, while not confined to the Adamanian or Revueltian, the pattern of fossil occurrences of *Typothorax* and *Paratypothorax* (Parker and Martz, 2011) suggests that these taxa originated sometime during the analytical time series. Inclusion in this analysis required that each taxon above meet three criteria:

1. Fossils must come from those Chinle localities where published U-Pb dates accommodate rigorous age estimation in Bchron (i.e. Petrified Forest National

Park, the *Placerias* Quarry, and the Hayden Quarry). Age constraints based on fossils or lithology, often established at those Chinle localities where geochronologic dates are unavailable, did not rise to the level of temporal precision permissible for the analysis.

2. The Alroy (2014) algorithm requires that each taxon have at least three fossil occurrences of different ages: two to define a temporal range, and at least one between them to define a frequency within that range. All taxa known from fewer than three total fossil occurrences at PEFO, the Placerias Quarry, and the Hayden Quarry were therefore excluded: these included *Tecovasuchus* (PFV 211), *Acallosuchus* (PFV 124), *Crosbysaurus* (PFV 122), and *Maleriasuchus* (PFV 161). *Rioarribasuchus* (PFV 075, PFV 366, and the Hayden Quarry) was also excluded on these grounds because the Bchron models frequently reconstructed two or more of these localities as contemporaneous, pushing the taxon below the analytical threshold.
3. Fossils must occur in localities correlable to U-Pb dated beds via continuously-exposed outcrop. Seventy-one PEFO fossil localities were included in this analysis, but fifteen additional localities that did not meet this criterion were excluded. General stratigraphic positions can be established for these additional localities per the stratigraphy of Martz and Parker (2010; see Parker and Martz, 2011); however, the uncertainty associated with those correlations—information required to integrate a locality into an age-depth model—cannot be tallied into a non-arbitrary cumulative term, as can those associated with correlations constructed along continuous outcrop.

Accordingly, *Scutarx deltatylus* (occurrences at PFV 224, PFV 169, PFV 304, and PFV 355, but the latter three cannot be correlated to dated beds with sufficient stratigraphic precision) and *Poposaurus* (occurrences at the *Placerias* Quarry, PFV 161, and PFV 336, but the last of these cannot be correlated with sufficient precision) were excluded from the analysis.

The Adamanian extinction was therefore defined as the intersection of the extinctions of *Acaenasuchus geoffreyi*, *Trilophosaurus*, *Calyptosuchus wellesi*, *Placerias hesternus*, *Desmatosuchus spurensis*, and *Smilosuchus*, and the Revueltian origination as the intersection of the originations of *Machaeroprosopus*, *Chindesaurus bryansmalli*, and *Revueltosaurus callenderi*. *Typothorax* and *Paratypothorax* were excluded from this analytical definition of the Revueltian origination because Adamanian-aged fossils belonging to these taxa exist. Table 2.7 lists voucher numbers for all fossils included in the analysis.

AGE-DEPTH MODELING IN BCHRON

A distribution of plausible ages was constructed for each PEFO fossil locality through age-depth modelling implemented in the R package Bchron (v. 4.3.0, Haslett and Parnell, 2008). Separate models for northern (Figure 2.1) and southern (Figure 2.2) PEFO were defined for practicality, as stratigraphic correlations can be most precisely drawn between U-Pb dates and those fossils situated closest geographically. Ages of fossils in northern PEFO were thus best determined with a model employing the date KWI (Devil's Playground, northern PEFO; Ramezani et al., 2011), and southern fossils with a model employing P-57C (Mountain Lion Mesa, southern PEFO; Nordt et al., 2015),

Inputs for the Bchronology function, used to build northern and southern PEFO age-depth models, are respectively available in Tables 2.1 and 2.2. Age inputs ("ages" and "ageSds" arguments) are scaled down by 10^3, but Bchronology scales them to their true magnitude as the ageScaleVal argument of the function defaults to 1000. Stratigraphic inputs ("position" and "thickness") are derived from the original field notes supporting the correlations of Ramezani et al. (2011), in addition to the positions Atchley et al. (2014) and Nordt et al. (2015) report for the dates SS-7 and P57-C. Because all ages are derived from a U-Pb isotopic system, the calibration curves ("calCurves") argument was set to "normal" following the instruction of Bchron documentation for non-14C ages. Each model was run for 1,000,000 iterations, with a burn-in period of 200,000 iterations and one iteration kept every 800 steps beyond the burn-in. Diagnostics (convergence checks and posterior outlier probability by date) of the age models are available in Tables 2.3 and 2.4.

Ages for the *Placerias* and Hayden Quarries were estimated by sampling ages in Bchron from the dates AB0513-2 (Ramezani et al., 2014) and Hayden 2 (Irmis et al., 2011), respectively. This approach, by contrast to an age-depth model, was justified because these dates were sampled directly from fossiliferous beds at both localities. It should be noted, however, that additional fossiliferous horizons exist at the Hayden Quarry beyond that containing Hayden 2. It was thus assumed that the broad analytical uncertainty associated with that date ($\pm$ 0.7 Ma) encompasses the complete depositional age of the Hayden Quarry.

Ages were estimated for these localities first by passing the inputs given in Tables 2.5 and 2.6 to the function BchronCalibrate to calibrate the dates. The subsequent outputs were then passed to the function sampleAges to generate ages. BchronCalibrate was run with all arguments set to their default values, and sampleAges with the "n_sample" argument set to provide 1000 age estimates.

TABLES AND FIGURES

Table 2.1. Geochronologic data used for Bchron age-depth model of northern Petrified Forest National Park.

id	ages	ageSds	position	thickness	calCurves
BFB	209926	72	0	1.25	normal
GPU	213124	69	101.01	0.75	normal
KWI	213870	78	109.545	1.28	normal
GPL	218017	88	140.045	1.92	normal
SBJ	219317	80	154.32	0.37	normal
SS-7	220123	68	185.075	0.5	normal
TPS	223036	59	189.125	0.76	normal
SS-28	225185	79	241.075	0.5	normal

Table 2.2. Geochronologic data used for Bchron age-depth model of southern Petrified Forest National Park.

id	ages	ageSds	position	thickness	calCurves
BFB	209926	72	0	1.25	normal
GPU	213124	69	101.01	0.75	normal
P57-C	213630	130	109.575	0.5	normal
GPL	218017	88	140.045	1.92	normal
SBJ	219317	80	154.32	0.37	normal
SS-7	220123	68	185.075	0.5	normal
TPS	223036	59	189.125	0.76	normal
SS-28	225185	79	241.075	0.5	normal

Table 2.3. Diagnostics of northern Petrified Forest National Park age model.

Convergence check		Posterior outlier probability by date	
Item	p-value		
SS-28	0.01079	Date	Probability
BFB	0.04959		
Outlier 1	0.05388	BFB	0.011
KWI	0.05895		
GPU	0.06749	GPU	0.007
SBJ	0.10622		
RateVar	0.10981	KWI	0.009
Outlier 5	0.16353		
GPL	0.26781	GPL	0.017
Outlier 4	0.27108		
TPS	0.31382	SBJ	0.014
Outlier 7	0.33808		
Outlier 2	0.35450	SS-7	0.012
Outlier 8	0.35450		
Outlier 6	0.35820	TPS	0.008
RateMean	0.41734		
Outlier 3	0.42872	SS-28	0.007
SS-7	0.43179		

Table 2.4. Diagnostics of southern Petrified Forest National Park age-depth model.

Convergence check		Posterior outlier probability by date	
Item	p-value	Date	Probability
Outlier 7	0.01391		
TPS	0.01578		
Outlier 2	0.02498	BFB	0.010
GPL	0.03077		
SS-7	0.04116	GPU	0.011
Outlier 3	0.04132		
P57-C	0.10662	P57-C	0.008
SS-28	0.21414		
RateMean	0.29593	GPL	0.010
Outlier 6	0.29694		
RateVar	0.30071	SBJ	0.009
Outlier 4	0.30129		
Outlier 8	0.35820	SS-7	0.012
GPU	0.37987		
BFB	0.39042	TPS	0.011
SBJ	0.39612		
Outlier 1	0.42872	SS-28	0.014
Outlier 5	0.49709		

Table 2.5. Geochronologic data for modeling age of *Placerias* Quarry in Bchron.

id	ages	ageSds	position	calCurves
AB0513-2	219390	120	0	normal

Table 2.6. Geochronologic data for modeling age of Hayden Quarry in Bchron.

id	ages	ageSds	position	calCurves
Hayden 2	211900	700	0	normal

TABLE 2.7. Voucher specimens and associated fossil localities.

Taxon	Locality	Bchron model	Position in age-depth model (m)	Voucher #
Acaenasuchus geoffreyi (Aetosauria)	PFV122	Southern PEFO	190.44 ± 1.35	PEFO 20358
	PFV211	Southern PEFO	175.55 ± 2.54	PEFO 16621
	Placerias Quarry	*Placerias* Quarry	0.00	MNA V36668
Calyptosuchus wellesi (Aetosauria)	PFV111	Southern PEFO	203.13 ± 1.67	UCMP 126856
	PFV112	Southern PEFO	204.66 ± 2.02	UCMP 126854
	PFV161	Southern PEFO	170.98 ± 3.57	UCMP 139492
	PFV162	Southern PEFO	169.61 ± 1.81	UCMP 126844
	PFV165	Southern PEFO	164.51 ± 2.81	UCMP 126943
	PFV167	Southern PEFO	146.76 ± 3.3	UCMP 126882
	PFV396	Southern PEFO	204.39 ± 4.38	PEFO 38265
	PFV445	Southern PEFO	201.52 ± 4.33	PEFO 38612
Desmatosuchus spurensis (Aetosauria)	PFV113	Southern PEFO	185.945 ± 2.92	PEFO 5038
	PFV167	Southern PEFO	146.755 ± 3.30	UCMP 126885
	PFV178	Southern PEFO	127.275 ± 3.51	UCMP 126976
	PFV198	Southern PEFO	202.47 ± 5.56	PEFO 31177
	PFV202	Southern PEFO	190.47 ± 1.83	PEFO 23338
	PFV211	Southern PEFO	175.55 ± 2.54	*PEFO 38402
	PFV212	Southern PEFO	173.90 ± 1.62	PEFO 26668
	PFV267	Southern PEFO	161.03 ± 0.47	PEFO 34935
	Placerias Quarry	*Placerias* Quarry	0.00	UCMP 78748
Paratypothorax (Aetosauria)	PFV037	Northern PEFO	96.60 ± 1.32	UCMP 139486
	PFV071	Southern PEFO	71.19 ± 0.35	UCMP 139958
	PFV097	Northern PEFO	137.73 ± 1.32	UCMP 129995
	PFV167	Southern PEFO	146.755 ± 3.30	PEFO 35003
	PFV272	Southern PEFO	117.34 ± 1.82	PEFO 31206
	PFV366	Southern PEFO	101.76 ± 2.81	PEFO 35263
Typothorax coccinarum (Aetosauria)	PFV037	Northern PEFO	96.60 ± 1.32	PEFO 5039
	PFV040	Northern	19.91 ± 3.28	PEFO 36757

		PEFO		
	PFV060	Southern PEFO	91.83 ± 1.42	PEFO 34882
	PFV070	Southern PEFO	71.19 ± 0.35	PEFO 23388
	PFV071	Southern PEFO	71.19 ± 0.35	PEFO 34851
	PFV075	Southern PEFO	92.12 ± 2.14	PEFO 36779
	PFV089	Southern PEFO	112.69 ± 1.28	PEFO 34869
	PFV092	Southern PEFO	102.98 ± 3.99	PEFO 34214
	PFV094	Southern PEFO	105.35 ± 2.76	UCMP 126855
	PFV097	Northern PEFO	137.73 ± 1.32	PEFO 34918
	PFV121	Southern PEFO	173.87 ± 3.29	PEFO 34213
	PFV215	Northern PEFO	15.30 ± 2.97	PEFO 16668
	PFV227	Southern PEFO	113.06 ± 1.06	PEFO 35018
	PFV231	Northern PEFO	25.00 ± 2.30	PEFO 33980
	PFV268	Southern PEFO	117.845 ± 1.15	PEFO 26702
	PFV290	Southern PEFO	120.54 ± 2.35	PEFO 34884
	PFV295	Southern PEFO	107.77 ± 1.58	PEFO 34280
	PFV326	Northern PEFO	34.75 ± 1.49	PEFO 38654
	PFV349	Southern PEFO	93.24 ± 1.31	PEFO 34847
	PFV367	Northern PEFO	129.49 ± 0.97	PEFO 34918
	PFV371	Northern PEFO	97.75 ± 2.38	PEFO 35131
	Hayden Quarry	Hayden Quarry	0.00	GR 229
Machaeroprosopus (Phytosauria)	PFV037	Northern PEFO	96.60 ± 1.32	PEFO 5034
	PFV040	Northern PEFO	19.91 ± 3.28	UCMP 126726
	PFV042	Northern PEFO	28.79 ± 2.37	PEFO 31219
	PFV075	Southern PEFO	92.12 ± 2.14	UCMP 126993
	PFV271	Southern PEFO	94.29 ± 1.81	PEFO 31205
	PFV295	Southern PEFO	107.77 ± 1.58	PEFO 31207
Smilosuchus (Phytosauria)	PFV097	Northern PEFO	137.73 ± 1.32	UCMP 26688
	PFV098	Northern PEFO	133.43 ± 1.19	UCMP 27181a
	PFV113	Southern PEFO	185.95 ± 2.92	UCMP 139554
	PFV122	Southern PEFO	190.44 ± 1.34	PEFO 5083
	PFV150	Southern PEFO	165.23 ± 2.29	PEFO 34869

	PFV142	Southern PEFO	201.61 ± 5.40	PEFO 31156
	PFV161	Southern PEFO	170.98 ± 3.57	PEFO 34921
	PFV177	Southern PEFO	129.49 ± 2.54	UCMP 129809
	PFV178	Southern PEFO	127.28 ± 3.51	PEFO 34866
	PFV182	Southern PEFO	201.055 ± 1.38	PEFOF 26682
	PFV268	Southern PEFO	117.845 ± 1.15	PEFO 31203
Chindesaurus bryansmalli (Dinosauria)	PFV018	Northern PEFO	21.12 ± 1.04	PEFO 4849
	PFV020	Northern PEFO	29.15 ± 0.51	PEFO 10395
	PFV089	Southern PEFO	112.69 ± 1.28	PEFO 34875
	PFV231	Northern PEFO	25.00 ± 2.30	PEFO 33982
	PFV332	Northern PEFO	23.67 ± 7.62	PEFO 34583
	Hayden Quarry	Hayden Quarry	0.00	GR 226
Revueltosaurus callenderi (Archosauria)	PFV040	Northern PEFO	19.91 ± 3.28	PEFO 34169
	PFV089	Southern PEFO	112.69 ± 1.28	PEFO 36759
	PFV215	Northern PEFO	15.30 ± 2.97	PEFO 16671
	PFV231	Northern PEFO	25.00 ± 2.30	PEFO 33991
	PFV297	Northern PEFO	22.98 ± 0.38	PEFO 33787
Trilophosaurus (Archosauria)	PFV122	Southern PEFO	190.44 ± 1.35	PEFO 3893
	PFV191	Southern PEFO	151.58 ± 1.21	PEFO 31165
	PFV396	Southern PEFO	204.39 ± 4.38	PEFO 38355
	Placerias Quarry	*Placerias* Quarry	0.00	UCMP 32390
Placerias hesternus (Dicynodonta)	PFV098	Northern PEFO	133.43 ± 1.19	UCMP 26682
	PFV113	Southern PEFO	185.945 ± 2.92	UCMP 139463
	PFV124	Southern PEFO	188.795 ± 2.29	UCMP 27095
	Placerias Quarry	*Placerias* Quarry	0.00	MNA PI 2770

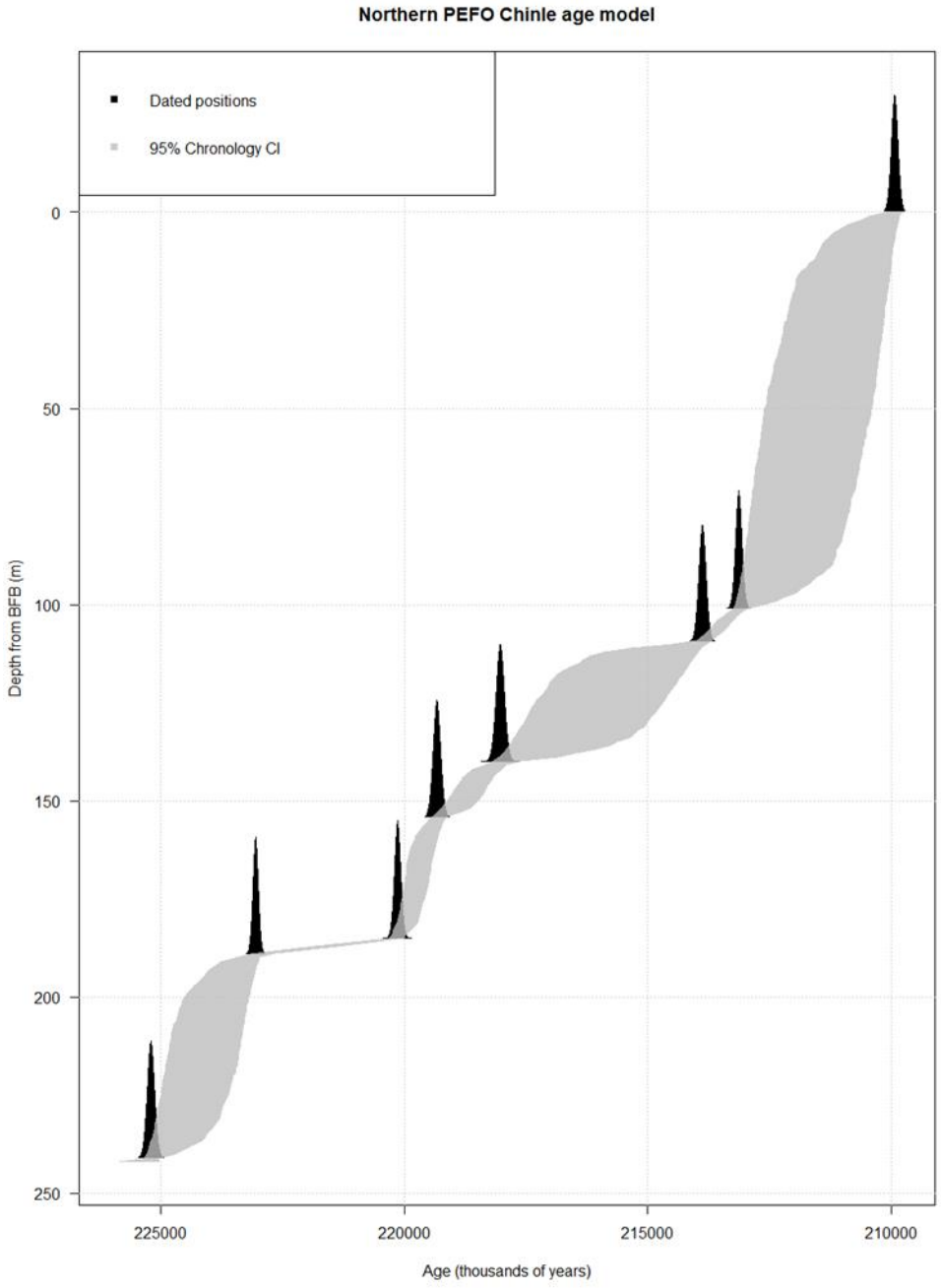

Figure 2.1. A Bayesian age-depth model of northern PEFO. Normal distributions (black) represent U-Pb dates, with width proportional to analytical uncertainty, while the grey field between them represents a 95% credible interval on the sedimentation history of the Chinle in PEFO. Temporal control over the system is proportional to the width of that field at a given stratigraphic level. Depth is given relative to the Black

Forest Bed (upper Petrified Forest Member), the source of the youngest U-Pb date in the model. A separate age model (Figure 2.2) is used for southern PEFO, differing only in the substitution of the date P57-C (213.63 ± 0.130 Ma) for KWI (213.87 ± 0.078 Ma). See Table 2.1 for model inputs, and Table 2.3 for diagnostics.

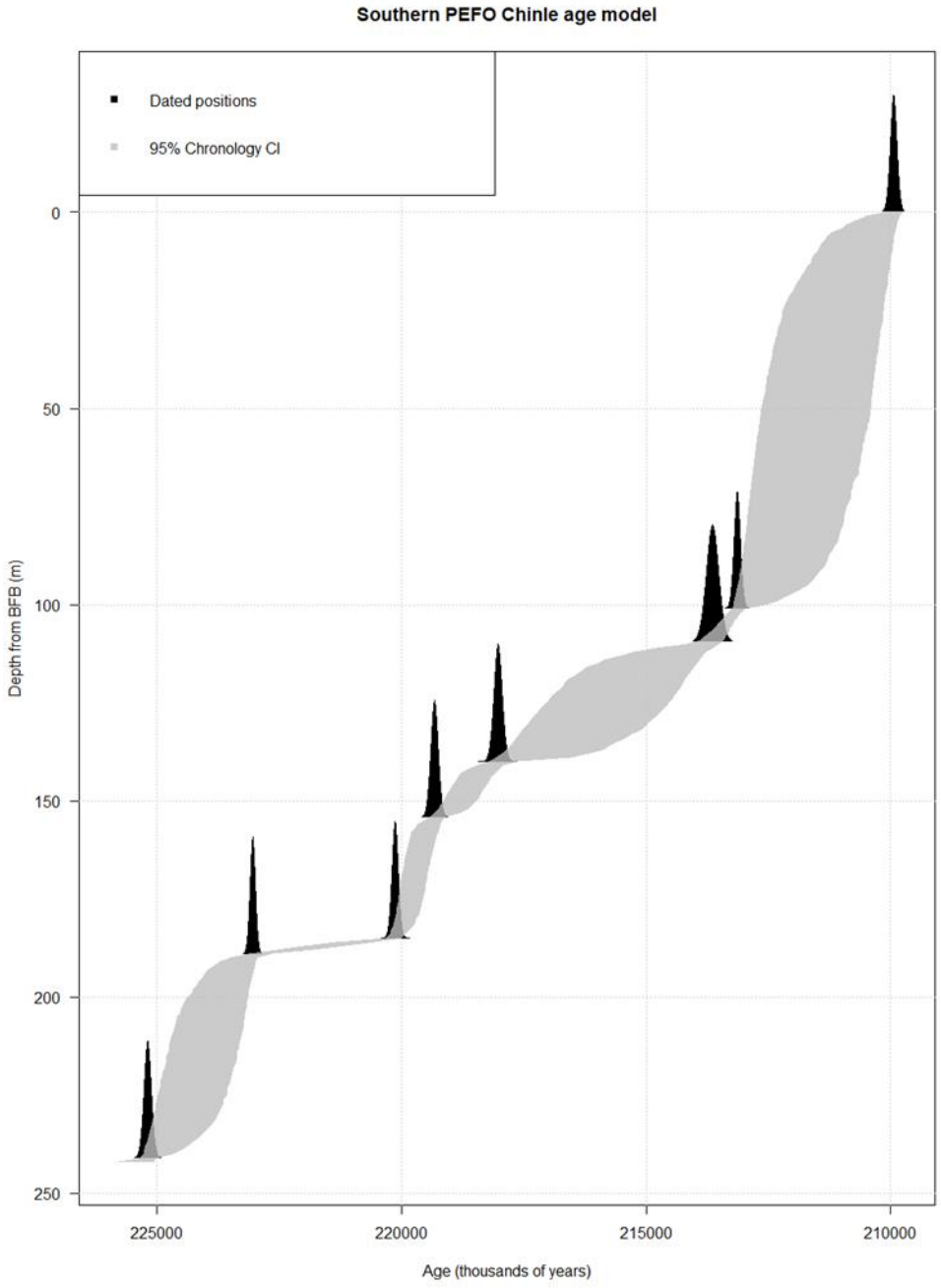

Figure 2.2. A Bayesian age-depth model of southern PEFO. Normal distributions (black) represent U-Pb dates, with width proportional to analytical uncertainty, while the grey field between them represents a 95% credible interval on the sedimentation history of the Chinle in PEFO. Temporal control over the system is proportional to the

width of that field at a given stratigraphic level. Depth is given relative to the Black Forest Bed (upper Petrified Forest Member), the source of the youngest U-Pb date in the model. A separate age model (Figure 2.1) is used for northern PEFO, differing only in the substitution of the date KWI (213.87 $\pm$ 0.078 Ma) for P57-C (213.63 $\pm$ 0.130 Ma). See Table 2.2 for model inputs, and Table 2.4 for diagnostics.

REFERENCES

Atchley S.C., Nordt L.C., Dworkin S.I., Ramezani J., Parker W.G., Ash S.R., and Bowring S.A., 2014, A linkage among Pangean tectonism, cyclic alluviation, climate change, and biologic turnover in the Late Triassic: The record from the Chinle Formation, southwestern United States: Journal of Sedimentary Research, v. 83, no. 12, p. 1147-1161, https://doi.org/10.2110/jsr.2013.89.

Haslett, J., and Parnell, A.C., 2008, A simple monotone process with application to radiocarbon-dated depth chronologies: Journal of the Royal Statistical Society: Series C (Applied Statistics), v. 57, no. 4, p. 399-418, https://doi.org/10.1111/j.1467-9876.2008.00623.x.

Gee, B.M. and Parker, W.G., 2017, A juvenile *Koskinonodon perfectus* (Temnospondyli, Metoposauridae) from the Upper Triassic of Arizona and its implications for the taxonomy of North American metoposaurids: Journal of Paleontology, v. 91, no. 5, p.1047-1059, https://doi.org/10.1017/jpa.2017.18

Gee, B.M., Parker, W.G., and Marsh, A.D., 2017, Microanatomy and paleohistology of the intercentra of North American metoposaurids from the Upper Triassic of Petrified Forest National Park (Arizona, USA) with implications for the taxonomy and ontogeny of the group: PeerJ, v. 5, p.e3183, https://doi.org/10.7717/peerj.3183.

Irmis, R.B., Nesbitt, S.J., Padian, K., Smith, N.D., Turner, A.H., Woody, D., and Downs, A., 2007, A Late Triassic dinosaurimorph assemblage from New Mexico and the rise of dinosaurs: Science, v. 317, p. 358-361, https://doi.org/10.1126/science.1143325.

Nordt, L., Atchely, S., and Dworkin, S., 2015, Collapse of the late Triassic megamonsoon in western equatorial Pangea, present-day American Southwest: Geological Society of America Bulletin, v. 127, no. 11-12, p. 1798 – 1815, https://doi.org/10.1130/b31186.1.

Parker, W.G., and Martz, J.W., 2011, The Late Triassic (Norian) Adamanian-Revueltian tetrapod faunal transition in the Chinle Formation of Petrified Forest National Park, Arizona: Earth and Environmental Science Transactions of the Royal Society of Edinburgh, v. 101, no. 3–4, p. 231–260, https://doi.org/10.1017/s1755691011020020.

Ramezani, J., Fastovsky, D.E., and Bowring, S.A., 2014, Revised chronostratigraphy of the lower Chinle Formation strata in Arizona and New Mexico (USA): High-precision U-Pb geochronological constraints on the Late Triassic evolution of dinosaurs: American Journal of Science, v. 314, p. 981-1008, https://doi.org/10.2475/06.2014.01.